Synthesis and Crystallization Behavior of Segmented Copolyesters/Silica Composites

Yun Hui Zhao, Li-Li Li, Xu-Bo Yuan, Jing Sheng

School of Materials Science and Engineering, Tianjin University, Tianjin 300072, People's Republic of China

Received 14 July 2005; accepted 9 January 2006
DOI 10.1002/app.24198
Published online in Wiley InterScience (www.interscience.wiley.com).

ABSTRACT: Silica were introduced to segmented copolyester system (poly(butylene terephthalate)-poly(ethylene terephthalate-*co*-isophthalate-*co*-sebacate) (PBT-PETIS)) by *in situ* polymerization. Investigations on melting behavior and crystalline structure were undertaken, and the dispersion situation of silica in segmented copolyester composites was detected. A diverse crystallization characteristic has been found when the modified Avrami analytical method was applied to investigate nonisothermal crystallization behavior of the composites. Crystallization rate was restricted rather than be promoted by increasing loading of silica. The values of Avrami exponent ranged from 2.25 to 2.45, presenting a mechanism of three-dimensional spherulitic growth with heterogeneous nucleation.
 J Appl Polym Sci 102: 1052–1058, 2006

Key words: polyesters; silica; composites; crystallization

INTRODUCTION

Polymer nanocomposites are of increasing importance because properties of polymer composites are remarkably modified at very low content of filler. Because of the special feature, composites exhibit new and excellently improved behaviors.

Among the composites, preparation of polycondensates composites including polyimide–clay hybrid,[1] nylon6/clay,[2] and PET/layered silicate[3] have been studied intensively.

In previous works,[4,5] we have addressed synthesis and characterization of segmented copolyesters PBT–PETIS by employing bulk polyester poly(butylene terephthalate) (PBT) and ternary amorphous random copolyester poly(ethylene terephthalate-*co*-isophthalate-*co*-sebacate) (PETIS) by means of melting transesterification processing. Since segmented polymers with crystallizing segments possess unique morphology,[6] we are now currently introducing silica particles into the intermediate composition of the segmented copolyester, expecting to obtain outstanding properties. The process is carried out by *in situ* polymerization, in which silica are dispersed in monomer and then is polymerized using a technique similar to bulk polymerization.

As for polyester/inorganic particle composites, besides the effect on mechanical properties, the most important feature is its crystallization behavior, which can lead to the modification of crystalline and to the production of new copolyester materials.

In present research, we report silica dispersion situation in segmented copolyester PBT–PETIS composites, melting behavior, and crystalline structure of the composites. With respect to plain PBT–PETIS, investigations on nonisothermal crystallization behavior of its composites were undertaken by differential scanning calorimetry (DSC), and the modified Avrami approach was applied to the analysis of crystallization kinetics.

EXPERIMENTAL

Materials

Modified silica were achieved from Beijing University of Chemical Technology, and the average diameter is 30–90 nm. Plain PBT chips and 1,4-butanediol (BG) were kindly supplied by Yi Zheng Chemical Fiber Co., China. Dimethyl terephthalate (DMT), ethylene glycol (EG), isophthalate acid (IPA), sebacate acid (SA), and tetrabutyl orthotitanate (TBT) were all reagent grade and were used as received.

Characterization of silica

Silica were ground with potassium bromine pellets, and then pressed to thin slice. Fourier transform infrared spectroscopy (FTIR) was conducted on a Nicolet FT-IR05.

Correspondence to: J. Sheng (shengxu@public.tpt.tj.cn).

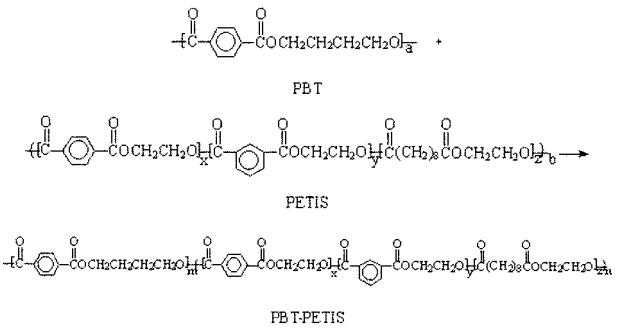

Scheme 1

Synthesis of PBT–PETIS/silica composites

Silica were dispersed in EG by ultrasonic vibration. Silica-dispersed EG was transesterified with DMT, and esterified with IPA and SA, respectively. The three products of transesterification and esterifications were employed to synthesize PETIS according to feed ratio in the presence of TBT as a catalyst. Polycondensation was carried out at (255 ± 2)°C in a four-neck flask equipped with a mechanically sealed stirrer and condenser under vacuum condition less than 133 Pa. Plain copolyester PETIS was fabricated by the same process without the addition of silica. Silica-dispersed BG was transesterified with DMT and then was polycondensated under vacuum condition as described already, and PBT composites were achieved.

Melting transesterification between PBT and PETIS with the same content of silica was conducted on the regular basis under nitrogen atmosphere and *in vacuo* condition. Melt processing was proceeded isothermally at (255 ± 2)°C for 20 min. The process is delineated in Scheme 1.

Characterization of PBT–PETIS/silica composites

The intrinsic viscosity of samples was determined at (25.0 ± 0.1)°C in a phenol/1,1,2,2-tetrachloroethane (50/50, (w/w)) solution with a concentration of 0.5 g/100 mL by a Ubbelohde viscometer. The density of polyesters was measured with a gradient density tube prepared according to ASTM-D1505 in a thermostat at (25.0 ± 0.1)°C using aqueous solution of sodium bromide. The ultramicrotomed sections of PBT–PETIS/silica composite were observed by a Philips EM400ST transmission electron microscope. X-ray diffraction measurement (XRD) was done on melt-pressed films in the reflection mode with a Rigaku diffractmeter using Ni-filtered Cu Kα radiation.

DSC procedures

A Shimadzu DSC-50 Differential Scanning Calorimetry was used for the measurements of melting and nonisothermal crystallization of polyesters. The apparatus is calibrated with Al_2O_3 under nitrogen atmosphere using samples of about 5 mg. The samples were heated up to predetermined temperatures, and maintained for 5 min. It was then cooled down with rate (R) of 2.5, 5, 10, and 20°C/min to room temperature, respectively.

The development of relative crystallinity with time dependence ($X(t)$) was obtained by integration of crystallization thermograms:

$$X(t) = \int_{t_0}^{t} \frac{dH}{dt} / \Delta H_c \qquad (1)$$

in which t_0 is the initial time when crystallization begins; $\int_{t_0}^{t} dH/dt$, the heat evolution rate at time t; and ΔH_c, the overall heat of crystallization.

RESULTS AND DISCUSSION

Synthesis and dispersion situation

Figure 1 shows the infrared spectrum of silica. The strong absorbance at 1099.5 cm^{-1} is attributed to the stretching of SiO_2. Moreover, two peaks are fitted to the stretching and bending of O—H at 3460 cm^{-1} and 1625 cm^{-1}, respectively.

The reason for choosing silica to synthesize polyester composites is that matching the polarity of particle with that of monomer is particularly critical to obtain good dispersion. Modified silica, with rich hydrophilic hydroxyl group-OH, is selected as an ideal candidate. By doing this, good dispersion is expected to be achieved at some extent because of the compatibility between hydroxyl group and hydrophilic monomers of ethylene glycol or 1,4-butanediol.

Designated samples with their intrinsic viscosity and density are shown in Table I. Filling PBT with silica increases the intrinsic viscosity by 32.15% for 1-PBT and 19.59% for 3-PBT, respectively. The elevation magnitude of intrinsic viscosity decreases as the content of silica is raised, which is mainly because higher concentration of filler does not favor dispersing silica to polymer matrix. Furthermore, physical or chemical constraint between silica and PBT molecules prevent the motion of main chain and the migration of monomers.

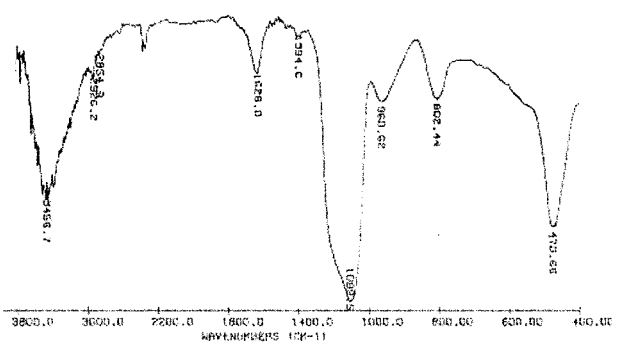

Figure 1 Infrared spectrum of silica.

TABLE I
Designated Samples with Their Intrinsic Viscosity and Density

Sample	Feed ratio (wt %) (PET/PEI/PES) = 40/20/40		Intrinsic viscosity (dL/g)	Density (g/cm^3)
	SiO_2	PBT/(PET/PEI/PES)		
PBT	0	100/(0/0/0)	0.8000	1.2795
1-PBT	1	100/(0/0/0)	1.0572	1.3165
3-PBT	3	100/(0/0/0)	0.9567	1.3251
PETIS	0	0/(40/20/40)	0.4866	1.2476
1-PETIS	1	0/(40/20/40)	0.6157	1.2490
3-PETIS	3	0/(40/20/40)	0.5871	1.2472
PBT–PETIS	0	30/(28/14/28)	0.5647	1.2637
1-(PBT–PETIS)	1	30/(28/14/28)	0.7338	1.2694
3-(PBT–PETIS)	3	30/(28/14/28)	0.7875	1.2664

Consequently polycondensation reaction stays at lower stage. Similar change of intrinsic viscosity is found in PETIS and PBT–PETIS. Meanwhile, density of PBT composites is somewhat raised, while the density is not found to be particularly influenced by the content of silica in PETIS and PBT–PETIS composites.

Figure 2 illustrates the dispersion situation of silica in segmented PBT–PETIS with the aid of transmission electron microscope. Silica particles can be well dispersed in segmented copolyester when the loading of filler is lower. In detail, copolyester with 1% silica by weight shows separate particles as well as aggregation with dimension of 100–200 nm, while there are aggregations on larger scale observed in sample with 3% silica. Liu et al.[7] believed that for high-concentration silica particles, the distance of the particles is small, so these particles are easy to aggregate. Visual observations of TEM demonstrate the analysis.

Melting behavior of PBT and PBT–PETIS composites

Table II summarized the characteristic data of melting and crystallization for PBT and its composites. The melting peaks are marked T_m, and ΔH_0 is the melting enthalpy. T_c and ΔH_c are the maximum and the enthalpy of exothermic peak, respectively. Moreover, the melting enthalpy for PBT composites are calibrated according to the actual mass of polymer in composites as follows:[8]

$$\Delta H_m = \frac{\Delta H_0}{1 - x} \tag{2}$$

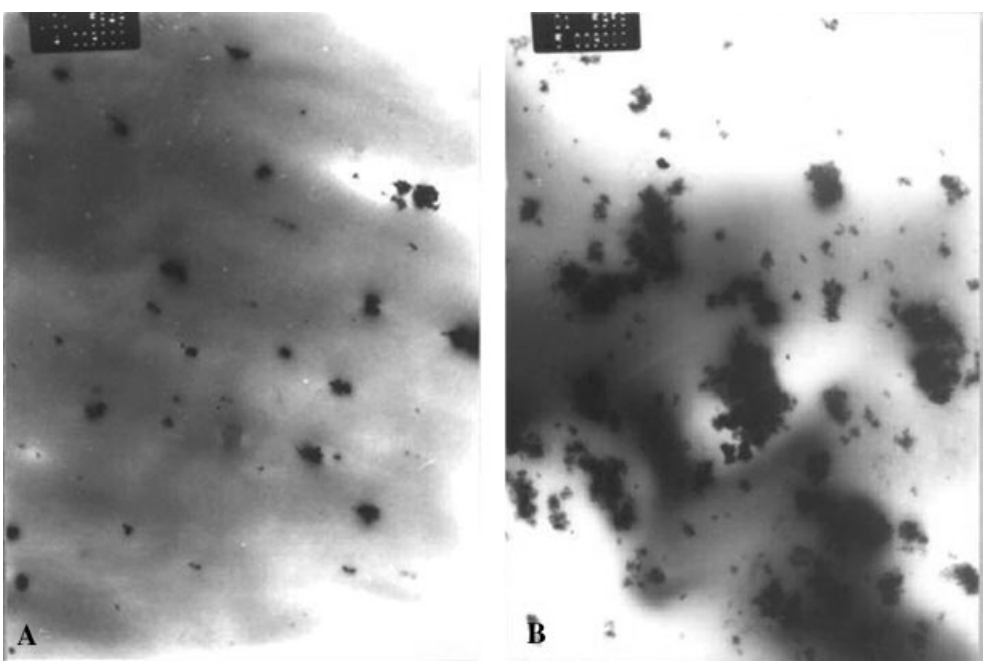

Figure 2 TEM micrographs of PBT–PETIS/silica composites (a) 1-(PBT–PETIS) (magnification: 9000×) (b) 3-(PBT–PETIS) (magnification: 9000×).

TABLE II
Characteristic Data of Melting and Crystallization for PBT and its Composites

Sample	T_m (°C)	$T_{m,\ onset}$ (°C)	$T_{m,\ endset}$ (°C)	ΔH_0 (J/g)	ΔH_m (J/g)	T_c (°C)	$T_{c,\ onset}$ (°C)	$T_{c,\ endset}$ (°C)	ΔH_c (J/g)
PBT	225.29	206.57	238.28	43.76	43.76	183.43	194.84	173.21	42.51
1-PBT	224.83	214.19	232.91	45.87	46.33	191.39	200.81	184.06	46.79
3-PBT	225.54	214.21	234.10	51.91	53.51	196.09	205.32	187.85	48.37

TABLE III
Characteristic Data of Melting Process for PBT-PETIS/Silica Composites

Sample	T_{m1} (°C)	T_{m2} (°C)	$T_{m,\ onset}$ (°C)	$T_{m,\ endset}$ (°C)	ΔH_0 (J/g)	ΔH_m (J/g)
PBT–PETIS	186.72	200.09	157.89	214.89	16.10	16.10
1-(PBT–PETIS)	180.80	193.49	145.31	212.27	15.12	15.27
3-(PBT–PETIS)	–	160.63	111.69	196.27	12.70	13.09

where ΔH_m is the melting enthalpy based on actual mass of polymer in composites, and x is the weight fraction of silica in samples.

The melting enthalpy ΔH_m increases profoundly and the peaks of melting and crystallization thermogram shifts to higher region as the loading of silica increases. It may be suggested that nucleated polyester has a higher regular crystalline structure than that of plain PBT. This is also adding justification for the rise of density.

The melting enthalpies that have been corrected according to eq. (2) for segmented copolyester PBT–PETIS (shown in Table III) are much lower than that of PBT. Furthermore, contrast to PBT composites, melting temperature of PBT–PETIS/silica composites gradually became lower when the content of silica is increased, and the melting enthalpies also decrease with the rise of silica content.

Since one of the outstanding features of segmented copolyesters is the domain nature to form a microphase separation,[9] their unique properties are largely from their two phases morphology. One of the phases is composed of crystallizable PBT, and the other is a homogeneous mixture of PETIS and noncrystallizable PBT.[10] The morphology model also suggests that PBT segments must be on average over a critical length to participate in crystallization.

Because PETIS is amorphous (which has been affirmed by DSC and XRD), the distribution of amorphous PETIS into PBT main chain by melting transesterification is the chief reason for the decrease of enthalpy. In PBT–PETIS/silica composites, it can be speculated that the effects of silica on composites are not straightforward. On one hand, silica serve as nucleating agent in PBT segments, leading to more perfect crystallization structure and rise of crystallinity. On the other hand, many of the longer, potentially crystallizable PBT segments are prevented from being incorporated into crystalline lattice because of the interaction between silica and the PBT molecules, which decreases the number of perfect crystallites. This trend seems to be significant when the load of silica is increased.

The nucleation effect would increase the crystallinity of segmented copolyester composites slightly when only a small portion of silica had an effect on the nucleation. However, most silica restricted the motion of the main chain of copolyesters because of the interaction.

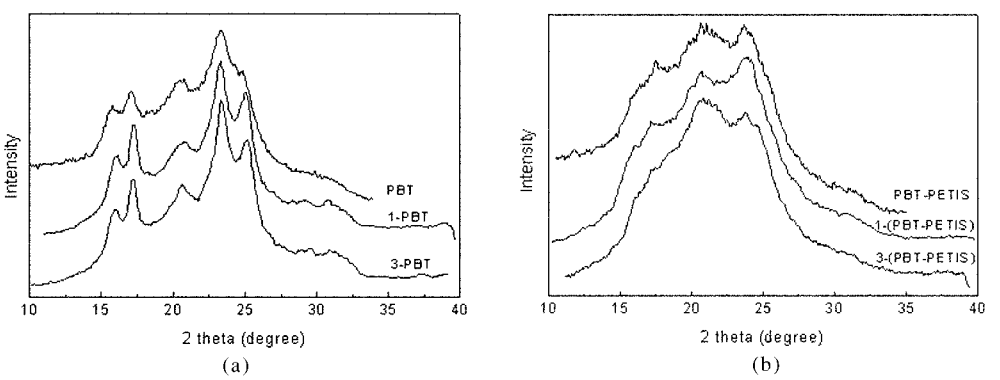

Figure 3 XRD patterns for PBT and PBT–PETIS samples (a) PBT (b) PBT–PETIS.

TABLE IV
Crystallography Data for PBT and PBT-PETIS Samples

	(010)			($\bar{1}$01)			(100)		
Sample	2θ (°)	β (°)	D (nm)	2θ (°)	β (°)	D (nm)	2θ (°)	β (°)	D (nm)
PBT	17.2	2.21	3.60	20.6	1.86	4.30	23.1	1.66	4.83
1-PBT	17.3	0.597	13.32	20.7	2.98	2.68	23.3	1.02	7.87
3-PBT	17.2	0.61	13.12	20.6	2.33	3.43	23.4	1.01	7.95
PBT–PETIS	17.5	3.29	2.42	20.4	2.11	3.79	23.5	3.57	2.25
1-(PBT–PETIS)	17.4	2.06	3.85	20.7	3.02	2.65	23.6	2.98	2.66
3-(PBT–PETIS)	17.4	3.32	2.39	20.6	2.44	3.27	23.7	3.13	2.53

The restricted chain cannot crystallize. When the hindrance of chain prevails over nucleation, the melting temperature and the melting enthalpy drop noticeably.

Crystalline structure

In the XRD patterns (Fig. 3) of PBT, five diffraction peaks, namely, 16.1, 17.2, 20.6, 23.1, and 25.2° are assigned for the (0$\bar{1}$1), (010), ($\bar{1}$01), (100), and (1$\bar{1}$1) plane, respectively. PBT and PBT–PETIS composites still exihibit the PBT-related scattering angles. A significant rise of intensity can be found in the patterns of PBT when silica is introduced. In comparison, diffraction peaks of PBT–PETIS samples are brodened obviously. Attempt has been made to divide patterns into separate Gaussian profiles, and then half-high breadth at the Bragg scattering angle (β) can be measured. By using Scherrer equation, crystallite dimensions (D) can be calculated (Table IV).

The crystallite dimensions of PBT composites are much larger than those of plain PBT especially for (010) and (100) planes. Returning again to consider the crystallinity, it can easily be deduced that the rise of crystallinity for PBT composites is caused not only by the effect of nucleation but also by the increase of crystallite dimension. All segmented PBT–PETIS samples, however, show smaller crystallite dimension in comparison with PBT, and the discrepancy between PBT–PETIS and PBT composites is more signigicant.

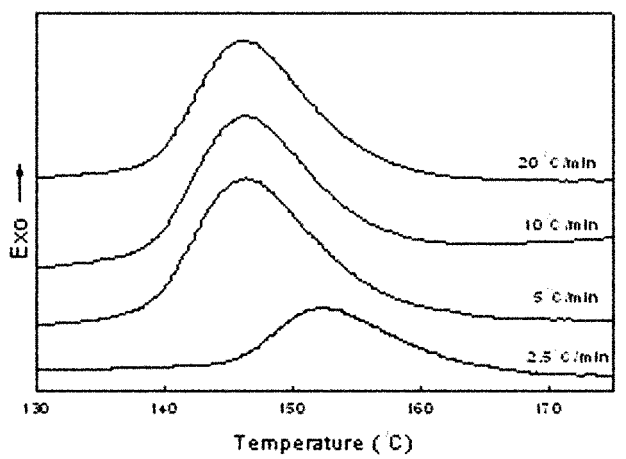

Figure 4 Crystallization exotherms for sample 1-(PBT–PETIS) measured at different cooling rates.

Nonisothermal crystallization behavior

The crystallization exotherms of sample 1-(PBT–PETIS) from the melt with four different cooling rates over 2.5–20.0°C/min are shown in Figure 4. The exothermic peaks shift to lower temperature region with increasing cooling rate. This observation has been found for plain PBT–PETIS and 3-(PBT–PETIS), and also a common phenomenon for semicrystalline polymer.[11–14] It is generally accepted that when polymer is undergoing crystallization at lower cooling rate, the segment motion can match the cooling rate and has relatively remains for a long time in the temperature range to promote rearrangement and crystallization. Table V summarizes the data of peak temperature (T_p), the time to reach maximum degree of crystalline order (t_p) as well as the crystallization enthalpies (ΔH_c). Moreover, crystallization temperature of PBT–PETIS became lower with the augment of silica contents at a given cooling rate.

Avrami equation[15–17] is known to describe isothermal crystallization kinetics of polymers successfully.

$$1 - X(t) = \exp(-Z_t t^n) \tag{3}$$

where n is the Avrami exponent whose value depends on the mechanism of nucleation and on the form of

TABLE V
Characteristic Data of Nonisothermal Crystallization Exotherms for Samples

Sample	R (°C/min)	T_p (°C)	t_p (min)	ΔH_c (J/g)
PBT–PETIS	20	145.32	1.88	14.34
	10	145.70	2.00	13.31
	5	145.30	2.25	15.94
	2.5	150.36	3.85	10.20
1-(PBT–PETIS)	20	146.09	2.20	13.86
	10	146.30	2.22	14.47
	5	146.41	2.32	11.17
	2.5	152.45	4.75	11.62
3-(PBT–PETIS)	20	126.99	3.08	10.04
	10	127.22	2.93	9.26
	5	127.33	3.32	9.69
	2.5	131.67	5.18	10.03

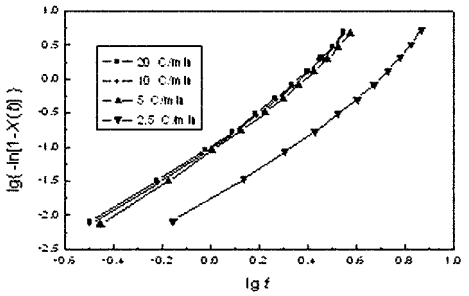

Figure 5 Avrami analysis based on the crystallization data for sample 1-(PBT–PETIS).

crystal growth, and Z_t is the crystallization kinetics constant containing the nucleation and the growth parameters.[18]

Nonisothermal crystallization has not been developed as fully as the isothermal approach but in attracting interest. The ultimate goal of the study on nonisothermal crystallization is a practical one of achieving parameters for real industrial processing. Many approaches[19–22] in obtaining applicable expression relating nonisothermal crystallization have been reported. A most promising one is to use the modified Avrami expression by taking the effect of cooling rate into consideration. The modified Avrami equation gives essentially the same expression, and the half-time of crystallization $t_{1/2}$ can be determined from the plots of relative crystallinity versus time.

Avrami lines obtained from following double logarithmic equation are presented in Figure 5:

$$\lg [-\ln(1 - X(t))] = \lg Z_t + n \lg t \tag{4}$$

The slop of the initial linear portion (n) and the antilogarithmic value of the intersection with y-axis (Z_t) can be calculated. Considering the cooling rate to be constant or approximately constant, Jeziorny[23] obtained the crystallization rate constant (Z_t) as follows:

TABLE VI
Kinetic Parameters from the Modified Avrami Analysis of Nonisothermal Crystallization

Sample	R (°C/min)	$t_{1/2}$ (min)	Z_c (min^{-n})	n
PBT–PETIS	20	1.83	0.90	2.44
	10	1.97	0.81	2.41
	5	2.25	0.61	2.35
	2.5	3.83	0.23	2.25
1-(PBT–PETIS)	20	2.04	0.89	2.40
	10	2.08	0.80	2.42
	5	2.21	0.62	2.45
	2.5	4.48	0.20	2.34
3-(PBT–PETIS)	20	2.82	0.87	2.32
	10	2.77	0.75	2.35
	5	3.14	0.53	2.39
	2.5	4.79	0.19	2.29

$$\lg Z_c = \lg Z_t/R \tag{5}$$

in which Z_c is the final form of crystallization rate constant, and R is the cooling rate. The values of $t_{1/2}$, n, and Z_c are collected in Table VI.

All Z_c values increase with increasing cooling rate while the values of $t_{1/2}$ are shortened, which indicates that crystallization rate is accelerated by increasing cooling rate. Since the nucleating capability of samples can be enhanced at rapid cooling rate, the increased nucleation density leads to the increase of crystallization rate, and a little time is needed for the development of crystalline entities.

There is a depression of crystallization rate by filling polymers with inorganic particle rather than increase the rate of crystallization as literatures mentioned.[24–26] For example, Z_c ranges from 0.23 to 0.90 min^{-n} for PBT–PETIS; from 0.20 min^{-n} to 0.89 min^{-n} for 1-(PBT–PETIS); from 0.19 min^{-n} to 0.87 min^{-n} for 3-(PBT–PETIS) in the order of increasing cooling rate. It is obvious that the crystallization rate of plain PBT–PETIS is numerically larger than its composites. The addition of silica hindered the molecules motion of copolyesters because of the interfacial tension. Moreover, the interaction generated from silica and molecules reduced the density of the nucleus and the migration ability of polyester to the nucleus. In this sense, it confirms our previous analysis of melting behavior. The negative influence of silica on crystallization rate of segmented PBT–PETIS composites is seemingly consistent with that of PP/starch composites system as literature provided early indication.[27]

In addition to the earlier-mentioned important results, meaningful coefficients consistent with other observation were obtained for the samples. The Avrami exponent (n) ranges from 2.25 to 2.45. It is evident from examining the known case of PBT[28] that there is a mechanism of three-dimensional spherulitic growth with heterogeneous nucleation. The same is true for segmented copolyester PBT–PETIS and its composites.

CONCLUSIONS

Segmented copolyesters PBT–PETIS/silica composites can be prepared by *in situ* polymerization. It shows good dispersion when silica content is lower, and the dispersion situation is getting worse with the increasing loading of silica. PBT–PETIS/silica composites exhibit lower value of melting temperature and melting enthalpy as well as smaller crystalline dimension. The modified Avrami analytical method is found to describe the nonisothermal crystallization of composites very well. Crystallization rate is restricted when the loading of silica is raised, which is different from that of other polymer/inorganic composites.

References

1. Yano, K.; Usuki, A.; Okada, A. J Polym Sci Part A: Polym Chem 1993, 31, 2493.
2. Liu, L. M.; Qi, Z. N.; Zhu, X. G. J Appl Polym Sci 1999, 71, 1133.
3. Yusuke, I.; Yoshinart, I.; Hiroshi, T. Polym J 2003, 35, 230.
4. Zhao, Y. H.; Sheng, J.; Wang, Y. Q. J Appl Polym Sci 2003, 87, 1232.
5. Zhao, Y. H.; Xu, G. H.; Jia, H. T.; Sheng, J. J Macromol Sci Pure Appl Chem 2003, 40, 461.
6. Niesten, M. C. E. J.; Krijgsman, J.; Harkema, S.; Gaymans, R. J. J Appl Polym Sci 2001, 82, 2194.
7. Liu, W. T.; Tian, X. Y.; Cui, P.; Li, Y.; Zheng, K.; Yang, Y. J Appl Polym Sci 2004, 91, 1229.
8. Ke, Y. C.; Long, C. F.; Qi, Z. N. J Appl Polym Sci 1999, 71, 1139.
9. Cella, R. J. J Polym Sci Polym Symp 1973, 42, 727.
10. Zhao, Y. H.; Xu, G. H.; Jia, H. T.; Sheng, J. J Polym Sci Part B: Polym Phys 2003, 41, 2257.
11. Liu, S. Y.; Yu, Y. N.; Cui, Y. J Appl Polym Sci 1998, 70, 2371.
12. Kong, X. H.; Yang, X. N.; Zhou, E. L. Eur Polym Mater 2000, 36, 1085.
13. Lee, S. W.; Lee, B.; Ree, M. Macromol Chem Phys 2000, 201, 453.
14. Lee, S. W.; Ree, M.; Park, C. E. Polymer 1999, 40, 7137.
15. Avrami, M. J Chem Phys 1939, 7, 1103.
16. Avrami, M. J Chem Phys 1940, 8, 212.
17. Avrami, M. J Chem Phys 1941, 9, 177.
18. Seo, Y.; Kim, J.; Kim, K. U. Polymer 2000, 41, 2639.
19. Tobin, M. C. J Polym Sci Part B: Polym Phys 1974, 12, 399.
20. Ozawa, T. Polymer 1971, 12, 150.
21. Ziabicki, A. Appl Polym Symp 1967, 6, 1.
22. An, Y.; Liu, T.; Dong, L.; Mo, Z. S.; Feng, Z. J Polym Sci Part B: Polym Phys 1998, 36, 1305.
23. Jeziorny, A. Polymer 1978, 19, 1142.
24. Cho, J. W.; Paul, D. R. Polymer 2001, 42, 1083.
25. Hasegava, N.; Okamoto, H.; Kato, M.; Usuki, A. J Appl Polym Sci 1978 2000, 78.
26. Tjong, S. C.; Li, R. K. Y.; Cheung, T. Polym Eng Sci 1997, 37, 166.
27. Liu, W. J.; Wang, Y. J.; Sun, Z. H. J Appl Polym Sci 2004, 92, 484.
28. Stein, R. S.; Misra, A. J Polym Sci Polym Phys Ed 1980, 18, 327.